Quarkonium dissociation in a thermal bath

Antonio Vairo

Physik-Department, Technische Universität München, James-Franck-Str. 1, 85748 Garching, Germany

Abstract. In an effective field theory framework we review the two main mechanisms of quarkonium dissociation in a weakly coupled thermal bath.

INTRODUCTION

Heavy particles may be sensitive to *new fundamental degrees of freedom* and serve as probes of new physics. Heavy particles themselves may appear as new fundamental degrees of freedom, an example discussed at this conference being heavy Majorana neutrinos [1]. Heavy particles, however, may also serve as probes of *new phenomena* emerging from particularly complex environments. We will focus on this second aspect here and discuss, in some special cases, how heavy quarkonia are affected by the hot medium formed in present-day heavy-ion colliders. At this conference, this has also been discussed elsewhere, for instance, in [2].

We consider a particle of mass M heavy, if M is much larger than any other energy scale E in the system. In particular, if M is also much larger than the momentum of the particle, this qualifies the particle as non-relativistic. The hierarchy of energy scales, $M \gg E$, allows an *effective field theory* (EFT) treatment at a scale μ such that $M \gg \mu \gg E$. The EFT describes the dynamics of the effective degrees of freedom that exist at the scale μ. These are the field H representing the low-energy fluctuations of the heavy particle, and all other low-energy fields. In a reference frame where the heavy particle is at rest up to fluctuations of order E or smaller, the EFT Lagrangian has the form

$$\mathscr{L} = H^\dagger i D_0 H + [\text{operators of dimension } d > 4] \times \frac{1}{M^{d-4}} + \mathscr{L}_{\text{light}}, \tag{1}$$

where $\mathscr{L}_{\text{light}}$ describes all low energy fields besides H. In the heavy-particle sector, the Lagrangian is organized as an expansion in $1/M$. Contributions of higher-order operators to physical observables are suppressed by powers of E/M. The EFT Lagrangian may be computed setting $E = 0$.

A special case is the case of a heavy particle of mass M in a medium characterized by a temperature T such that $M \gg T$. The system is described at a scale μ such that $M \gg \mu \gg T$ by an EFT Lagrangian that has the same structure as (1) if the heavy particle is at rest up to fluctuations of order T or smaller. This follows from the fact that the Lagrangian may be computed setting $T = 0$. In particular, the Wilson coefficients encoding the high-energy modes may be computed in vacuum. The Lagrangian is again organized as an expansion in $1/M$, whose higher-order contributions to physical observables are suppressed by powers of T/M.

Temperature is introduced via the partition function. Sometimes it is useful to work in the *real-time formalism*. Despite the fact that in real time the degrees of freedom double ("1" and "2"), the advantages are that the framework becomes very close to the one of $T = 0$ EFTs and that, in the heavy-particle sector, the second degrees of freedom, labeled "2", decouple from the physical degrees of freedom, labeled "1". This often leads to a simpler treatment with respect to alternative calculations in imaginary time formalism [3].

In the following, we will consider the special case of a heavy quarkonium, i.e., a bound state of a heavy quark Q and a heavy antiquark $\bar{Q}$, weakly bound, interacting with a weakly coupled plasma. This means that we consider a quarkonium sufficiently tight to be described as a *Coulombic bound state* (e.g. the bottomonium ground state) interacting with a medium sufficiently hot to behave as a *weakly coupled quark-gluon plasma* [4, 5]. We will compute thermal corrections to the width induced by the medium. We will call these, the quarkonium thermal width, Γ.

HEAVY QUARKONIA IN A THERMAL BATH

Lattice data suggest a crossover from hadronic matter to a plasma of deconfined quarks and gluons happening at a *critical temperature* $T_c = 154 \pm 9$ MeV [6]. High energy densities with temperatures larger than T_c are produced in heavy-ion collisions at RHIC and LHC. High-energy probes are needed to identify and qualify the state of matter that is formed there. Heavy quarkonium has been suggested as one of those probes [7]. This is because heavy quarks are formed early in heavy-ion collisions, heavy quarkonium formation will be sensitive to the medium and the dilepton signal makes an ideally clean experimental probe.

Quarkonium, being a composite system, is characterized by several energy scales [8]: M, Mv (momentum transfer, typical inverse distance), Mv^2 (kinetic energy, binding energy E_{binding}, potential V), ..., where v is the relative heavy-quark velocity; $v \sim \alpha_s$ for a Coulomb bound state. These in turn may be sensitive to thermodynamical scales smaller than the temperature. The thermodynamical scales are: πT, m_D (Debye mass, i.e. inverse screening length of the chromoelectric interactions), ... The non-relativistic scales are hierarchically ordered: $M \gg Mv \gg Mv^2$. In a weakly-coupled plasma one assumes this also to be the case for the thermodynamical scales: $\pi T \gg m_D \sim gT$. A weakly coupled quarkonium is the bottomonium ground state, $\Upsilon(1S)$; produced in heavy-ion experiments at the LHC it may possibly realize the hierarchy of energy scales [9, 10]: $M_b \approx 5$ GeV $> M_b \alpha_s \approx 1.5$ GeV $> \pi T \approx 1$ GeV $> M_b \alpha_s^2 \approx 0.5$ GeV $\sim m_D \gtrsim \Lambda_{\text{QCD}}$, for a temperature of the plasma of about 320 MeV $\approx 2T_c$. The existence of a hierarchy of energy scales calls for a description of the system (quarkonium at rest in a thermal bath) in terms of a hierarchy of EFTs. These are listed on the right arrow of Figure 1.
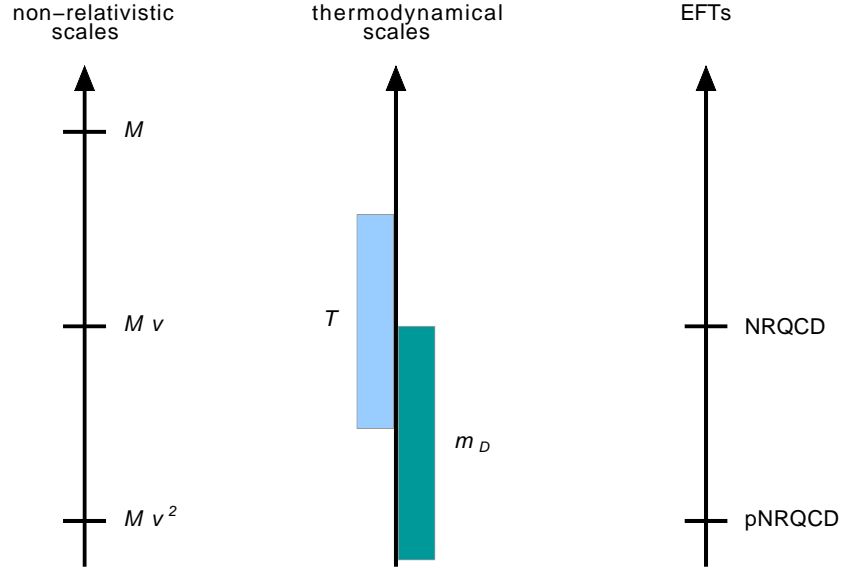

FIGURE 1.   Energy scales and EFTs relevant for a heavy quarkonium in a weakly-coupled quark-gluon plasma.

Non-relativistic QCD (NRQCD) is obtained by integrating out modes associated with the scale M [11, 12] and possibly with thermodynamical scales larger than Mv. The Lagrangian is organized as an expansion in $1/M$ and is of the form (1):

$$\mathscr{L} = \psi^\dagger \left(iD_0 + \frac{\mathbf{D}^2}{2M} + \dots \right) \psi + \chi^\dagger \left(iD_0 - \frac{\mathbf{D}^2}{2M} + \dots \right) \chi + \dots + \mathscr{L}_{\text{light}}, \qquad (2)$$

where ψ (χ) is the field that annihilates (creates) the (anti)fermion.

Potential non-relativistic QCD (pNRQCD) is obtained by integrating out modes associated with the scale Mv [13, 14] and possibly with thermodynamical scales larger than Mv^2. The degrees of freedom of pNRQCD are quark-antiquark states (color singlet S, color octet O), low energy gluons and light quarks propagating in the medium. The

Lagrangian is organized as an expansion in $1/M$ and r, the distance between the heavy quark and antiquark,

$$\mathscr{L} = \int d^3r \, \mathrm{Tr} \left\{ \mathrm{S}^\dagger \left(i\partial_0 + \frac{\nabla_r^2}{M} - V_s + \dots \right) \mathrm{S} + \mathrm{O}^\dagger \left(iD_0 + \frac{\nabla_r^2}{M} - V_o + \dots \right) \mathrm{O} \right\}$$

$$+ \mathrm{Tr} \left\{ \mathrm{O}^\dagger \mathbf{r} \cdot g\mathbf{E}\,\mathrm{S} + \mathrm{H.c.} \right\} + \frac{1}{2} \mathrm{Tr} \left\{ \mathrm{O}^\dagger \mathbf{r} \cdot g\mathbf{E}\,\mathrm{O} + \mathrm{c.c.} \right\} + \dots + \mathscr{L}_{\mathrm{light}}, \tag{3}$$

where V_s and V_o are the quark-antiquark colour-singlet and colour-octet potentials respectively, and $\mathbf{E}$ is the chromo-electric field. The term $\mathscr{L}_{\mathrm{light}}$ in the NRQCD and pNRQCD Lagrangians describes the (in-medium) propagation of gluons and light quarks.

Dissociation

A quantity that may be relevant for describing the observed quarkonium dilepton signal emerging from heavy-ion collisions is the *quarkonium thermal dissociation width*. Two distinct dissociation mechanisms may be identified at leading order: *gluodissociation*, which is the dominant mechanism for temperatures such that $m_D \ll Mv^2$, *dissociation by inelastic parton scattering*, which is the dominant mechanism for temperatures such that $m_D \gg Mv^2$. Beyond leading order the two mechanisms become intertwined and a distinction between them less practical.
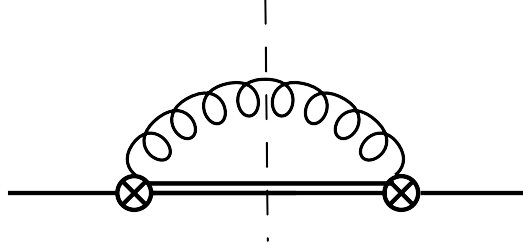

FIGURE 2. pNRQCD cutting diagram responsible for gluodissociation at leading order. In a pNRQCD Feynman diagram, single lines stand for quark-antiquark colour singlet propagators, double lines for colour octet propagators, curly lines for gluons and a circle with a cross for a chromoelectric dipole vertex.

Gluodissociation is the dissociation of quarkonium induced by the absorption of a gluon from the medium [15, 16]. The exchanged gluon is lightlike or timelike. The process happens when the gluon has an energy of order Mv^2, therefore it may be described at the level of pNRQCD by the cutting diagram shown in Figure 2. For a quarkonium at rest with respect to the medium, the dissociation width can be written as

$$\Gamma_{nl} = \int_{q_{\mathrm{min}}} \frac{d^3q}{(2\pi)^3} n_{\mathrm{B}}(q) \, \sigma_{\mathrm{gluo}}^{nl}(q), \tag{4}$$

where $\sigma_{\mathrm{gluo}}^{nl}$ is the in-vacuum cross section $(Q\overline{Q})_{nl} + g \to Q + \overline{Q}$, and n_{B} the Bose–Einstein distribution. Gluodissociation is also known as *singlet-to-octet break up* [3].

Dissociation by inelastic parton scattering is the dissociation of quarkonium by scattering with gluons and light-quarks in the medium [17, 18]. The exchanged gluon is spacelike. In the NRQCD Lagrangian each transverse gluon is suppressed by T/M (see (2)), hence at leading order one just needs to consider diagrams with one exchanged gluon. If the exchanged momentum is of order Mv, then dissociation by inelastic parton scattering is described at the level of NRQCD by the cutting diagrams shown in Figure 3. If the exchanged momentum is of order Mv^2, then it is described at the level of pNRQCD by the cutting diagram shown in Figure 4. For a quarkonium at rest with respect to the medium, the thermal width has the form [19]

$$\Gamma_{nl} = \sum_p \int_{q_{\mathrm{min}}} \frac{d^3q}{(2\pi)^3} f_p(q) \left[1 \pm f_p(q) \right] \sigma_p^{nl}(q), \tag{5}$$

where the sum runs over the different incoming and outcoming light partons p ($p = g$ for gluons with the plus sign, and $p = q$ for quarks with the minus sign), $f_g(q) = n_{\mathrm{B}}(q) = 1/(e^{q/T} - 1)$ and $f_q(q) = n_{\mathrm{F}}(q) = 1/(e^{q/T} + 1)$. The
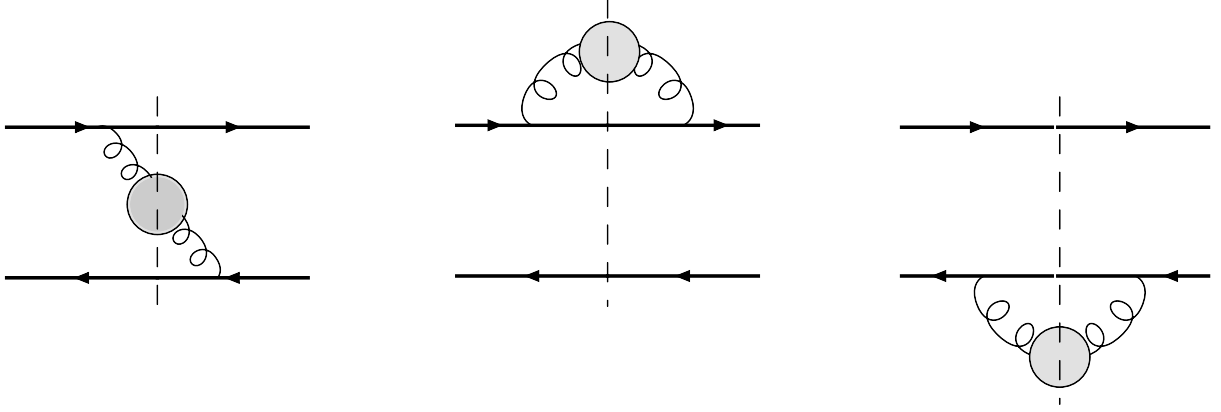
FIGURE 3. NRQCD cutting diagrams responsible for dissociation by inelastic parton scattering at leading order. In a NRQCD Feynman diagram, single lines stand for quark or antiquark propagators. The shaded blobs represent gluon self-energy diagrams.

cross section σ_p^{nl} may be identified with the in-medium cross section $(Q\overline{Q})_{nl} + p \rightarrow Q + \overline{Q} + p$. We observe that the formula differs from the gluodissociation formula (4), a point not always appreciated by the literature on the subject. Dissociation by inelastic parton scattering is also known as *Landau damping* [20].
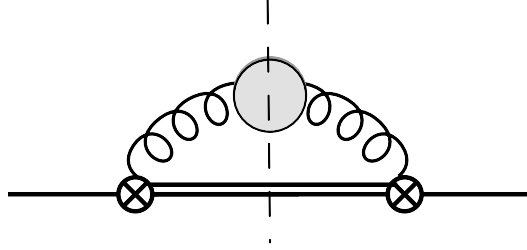

FIGURE 4. pNRQCD cutting diagram responsible for dissociation by inelastic parton scattering at leading order.

We define the quarkonium *dissociation temperature* as the temperature at which $\Gamma \sim E_{\text{binding}}$ and the *screening temperature* as the temperature at which $1/m_D$ is of the order of the quarkonium Bohr radius. At weak coupling, it holds that $\pi T_{\text{dissociation}} \sim Mg^{4/3}$ and $\pi T_{\text{screening}} \sim Mg$. This implies that $T_{\text{screening}} \gg T_{\text{dissociation}}$. In the special case of the $\Upsilon(1S)$, $T_{\text{dissociation}}$ has been estimated to be about 450 MeV [21], which implies that $T \approx 320$ MeV is below the dissociation temperature.

In the following, we will consider different temperature regimes below the dissociation (and hence the screening) temperature and above the critical temperature [19]. For these regimes we will provide the dissociation cross sections for a quarkonium that is a Coulombic $1S$ bound state. The wave function is $\langle \mathbf{r}|1S \rangle = 1/(\sqrt{\pi} a_0^{3/2}) \exp(-r/a_0)$, $a_0 = 2/(MC_F\alpha_s)$ the Bohr radius, $C_F = (N_c^2 - 1)/(2N_c) = 4/3$ and $N_c = 3$ the number of colours.

The temperature region $T \gg Mv \gg m_D$

In the temperature region $T \gg Mv \gg m_D$ the $1S$ dissociation cross section by parton scattering is

$$\sigma_p^{1S} = \sigma_{cp} f(m_D a_0), \tag{6}$$

where

$$\sigma_{cq} \equiv 8\pi C_F n_f \alpha_s^2 a_0^2, \tag{7}$$

$$\sigma_{cg} \equiv 8\pi C_F N_c \alpha_s^2 a_0^2, \tag{8}$$

$$f(m_D a_0) \equiv \frac{2}{(m_D a_0)^2} \left[1 - 4 \frac{(m_D a_0)^4 - 16 + 8(m_D a_0)^2 \ln\left(4/(m_D a_0)^2\right)}{((m_D a_0)^2 - 4)^3} \right], \tag{9}$$

and n_f is the number of light quarks. The cross section is not related, even at leading order, with a zero temperature process. The underlying reason is the infrared (IR) sensitivity of the cross section at the momentum scale Mv. This IR sensitivity is cured by the hard-thermal loop resummation at the scale m_D and signaled by the logarithm $\ln(m_D a_0)$. The cross section is momentum independent.

The *quasi-free approximation* amounts at replacing σ_p^{nl} by $2\sigma_p^Q$, where σ_p^Q is the in-vacuum cross section $p + Q \rightarrow p + Q$. Hence the quasi-free approximation is equivalent to neglecting interference terms between the different heavy-quark lines in the amplitude square. Interference terms are the ones sensitive to the bound state. This corresponds in approximating $f(m_D a_0) \approx 2/(m_D a_0)^2$. The approximation holds only for $m_D \gg 1/a_0$, but at these temperatures quarkonium is dissociated. For lower temperatures the approximation is largely violated by bound-state effects, see Figure 5.
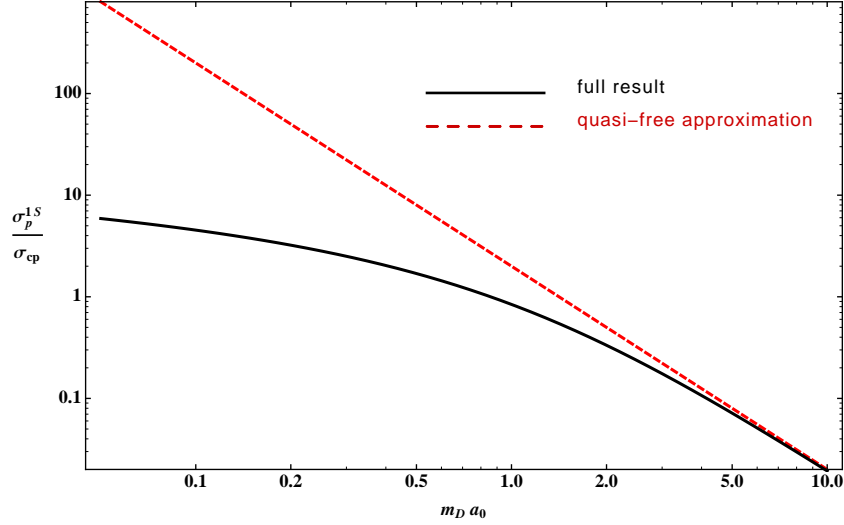

FIGURE 5. The cross section $\sigma_p^{1S}/\sigma_{cp}$ as a function of $m_D a_0$. The continuous line corresponds to the exact result, whereas the red dashed line corresponds to the quasi-free approximation.

The temperature region $T \sim Mv \gg m_D$

In the temperature region $T \sim Mv \gg m_D$ the $1S$ dissociation cross section by parton scattering is

$$\sigma_p^{1S} = \sigma_{cp}\, h_p(m_D a_0, q a_0), \tag{10}$$

where

$$h_q(m_D a_0, q a_0) \equiv -\ln\left(\frac{(m_D a_0)^2}{4}\right) - \frac{3}{2} + \ln\left(\frac{(q a_0)^2}{1 + (q a_0)^2}\right) - \frac{1}{2(q a_0)^2}\ln(1 + (q a_0)^2), \tag{11}$$

$$h_g(m_D a_0, q a_0) \equiv -\ln\left(\frac{(m_D a_0)^2}{4}\right) - \frac{3}{2} + \ln\left(\frac{(q a_0)^2}{1 + (q a_0)^2}\right) + \frac{1}{2(1 + (q a_0)^2)} - \frac{1}{(q a_0)^2}\ln(1 + (q a_0)^2). \tag{12}$$

The cross section is momentum dependent.

The temperature region $Mv \gg T \gg m_D \gg Mv^2$

In the temperature region $Mv \gg T \gg m_D \gg Mv^2$ the $1S$ dissociation cross section by parton scattering is given by

$$\sigma_p^{1S}(q) = \sigma_{cp}\left[\ln\left(\frac{4q^2}{m_D^2}\right) - 2\right]. \tag{13}$$
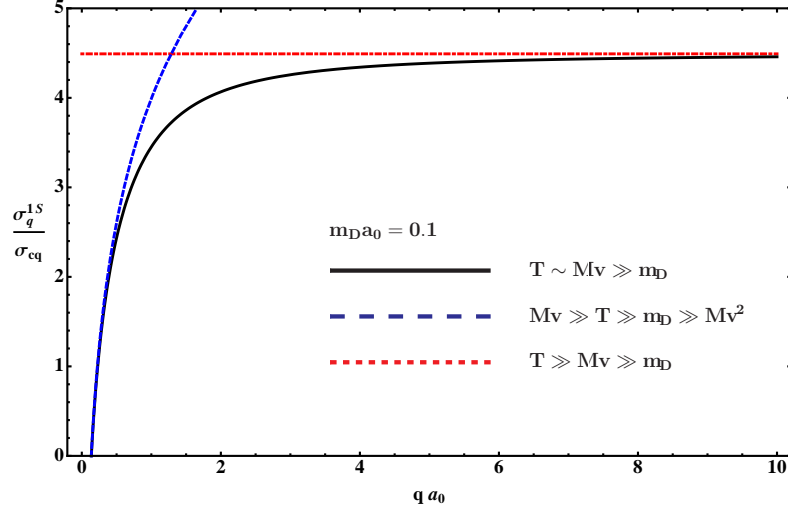
FIGURE 6. Dissociation cross sections due to scattering with light quarks, $\sigma_q^{1S}/\sigma_{cq}$, as a function of qa_0. The dashed blue curve shows the cross section for $Mv \gg T \gg m_D \gg Mv^2$, the continuous black curve shows the cross section for $T \sim Mv \gg m_D$, and the dot-dashed red curve shows the cross section for $T \gg Mv \gg m_D$; for all the curves $m_D a_0 = 0.1$.
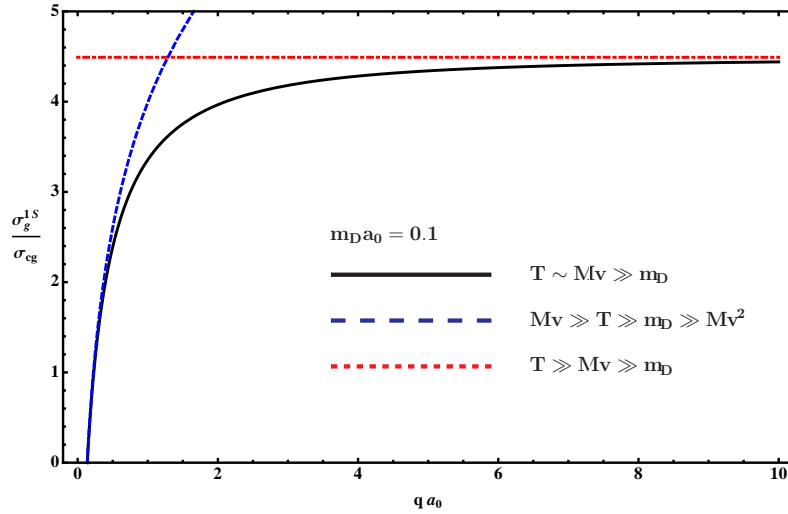

FIGURE 7. Dissociation cross sections due to scattering with gluons, $\sigma_g^{1S}/\sigma_{cg}$, as a function of qa_0. The dashed blue curve shows the cross section for $Mv \gg T \gg m_D \gg Mv^2$, the continuous black curve shows the cross section for $T \sim Mv \gg m_D$, and the dot-dashed red curve shows the cross section for $T \gg Mv \gg m_D$; for all the curves $m_D a_0 = 0.1$.

The cross sections due to inelastic scatterings with quarks and gluons in the three different regimes are summarized in Figures 6 and 7 respectively [19]. The thermal width follows from (5) and is displayed in Figure 8 [22].

The temperature region $Mv \gg T \gg Mv^2 \gg m_D$

In the temperature region $Mv \gg T \gg Mv^2 \gg m_D$, gluodissociation becomes such a competitive dissociation process to dominate, at least parametrically, over the dissociation by parton scattering.
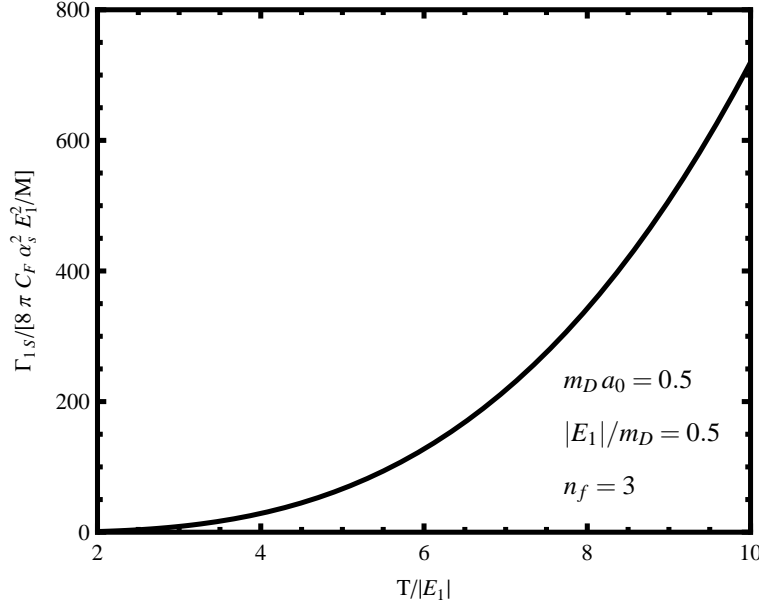
FIGURE 8. Thermal width due to inelastic parton scattering. We have integrated over the continuous black curves shown in Figures 6 and 7 and summed over all partons according to (5).

In fact, the $1S$ dissociation cross section by parton scattering is in this regime

$$\sigma_p^{1S}(q) = \sigma_{cp} \left[\ln\left(\frac{4q^2}{m_D^2}\right) + \ln 2 - 2 \right], \tag{14}$$

which induces a thermal width of order $\alpha_s T \times (m_D/Mv)^2$.

The $1S$ gluodissociation cross section is at leading order

$$\sigma_{\mathrm{gluo\,LO}}^{1S}(q) = \frac{\alpha_s C_F}{3} 2^{10} \pi^2 \rho(\rho+2)^2 \frac{E_1^4}{Mq^5} \left(t(q)^2 + \rho^2\right) \frac{\exp\left(\frac{4\rho}{t(q)}\arctan(t(q))\right)}{e^{\frac{2\pi\rho}{t(q)}} - 1}, \tag{15}$$

where $\rho \equiv 1/(N_c^2 - 1)$, $t(q) \equiv \sqrt{q/|E_1| - 1}$ and $E_1 = -MC_F^2\alpha_s^2/4$ [23, 24]. This cross section induces a thermal width of order $\alpha_s T \times (Mv^2/Mv)^2$, i.e., larger by a factor $(Mv^2/m_D)^2$ than the dissociation width by inelastic parton scattering. In this regime, gluodissociation is indeed the dominant dissociation mechanism.

Of the same order as the dissociation by parton scattering is the gluodissociation at next-to-leading order, which has been calculated in [19]. The gluodissociation cross section up to next-to-leading order reads

$$\sigma_{\mathrm{gluo}}^{1S}(q) = Z(q/m_D)\,\sigma_{\mathrm{gluo\,LO}}^{1S}(q), \tag{16}$$

$$Z(q/m_D) = 1 - \frac{m_D^2}{4q^2}\left[\ln(8q^2/m_D^2) - 2\right]. \tag{17}$$

The result follows from adding a gluon self-energy diagram to the gluon propagator before or after the cut in Figure 2. A comparison between the gluodissociation cross sections up to leading and next-to-leading order is in Figure 9.

The *Bhanot–Peskin approximation* is a largely used approximation of the exact gluodissociation formula (15) that consists in neglecting final state interactions, i.e. the rescattering of a $Q\overline{Q}$ pair in a color octet configuration [25, 26]. Because the quark-antiquark colour-octet potential is $V_o = 1/(2N_c) \times \alpha_s/r$, it vanishes in the large N_c limit:

$$\sigma_{\mathrm{gluo\,LO}}^{1S}(q) \xrightarrow[N_c\to\infty]{} 16\frac{2^9\pi\alpha_s}{9}\frac{|E_1|^{5/2}}{m}\frac{(q+E_1)^{3/2}}{q^5} = 16\,\sigma_{\mathrm{BP}}^{1S}(q), \tag{18}$$

$$\Gamma_{1S\mathrm{LO}} \xrightarrow[N_c\to\infty]{} \int_{q\geq|E_1|} \frac{d^3q}{(2\pi)^3} n_\mathrm{B}(q)\,16\,\sigma_{\mathrm{BP}}^{1S}(q) = \Gamma_{1S,\mathrm{BP}}, \tag{19}$$
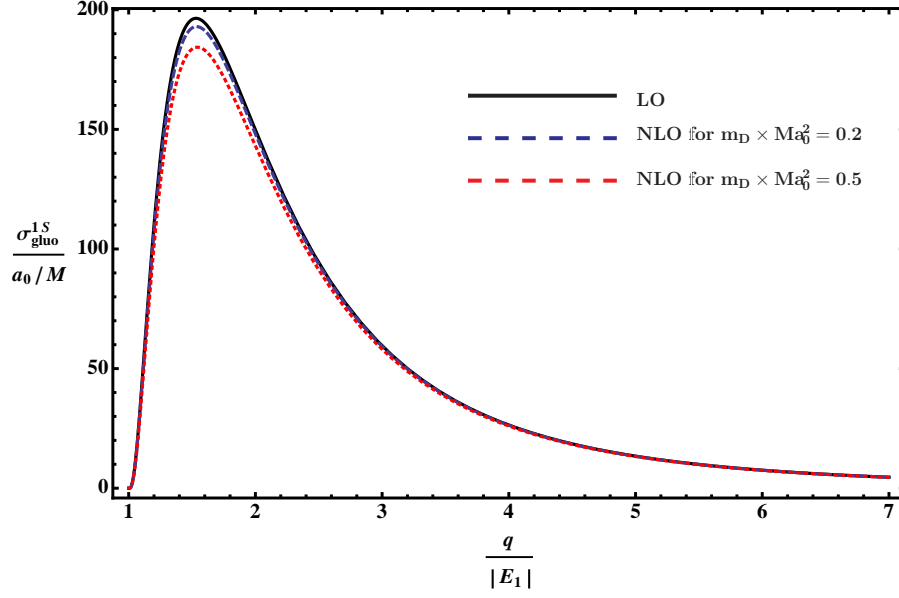
FIGURE 9. $1S$ gluo-dissociation cross section at leading order (continuous black line) and up to next-to-leading order for $m_D M a_0^2 = 0.2$ (dashed blue line) and for $m_D M a_0^2 = 0.5$ (dotted red line).

where we have kept $C_F = 4/3$ in the overall normalization and $E_1 = -MC_F^2 \alpha_s^2/4$. The cross section σ_{BP}^{1S} and the width $\Gamma_{1S,BP}$ are respectively the cross section and the width in the Bhanot–Peskin approximation. A comparison of the exact width with the Bhanot–Peskin width is in Figure 10 [23]. At high temperatures, the exact width is about 13% larger than its approximation, which is consistent with the large N_c limit. At low temperatures the thermal width goes to zero, however the exact and approximate widths vanish with different functional behaviours and the approximate width largely overshoots the exact one.
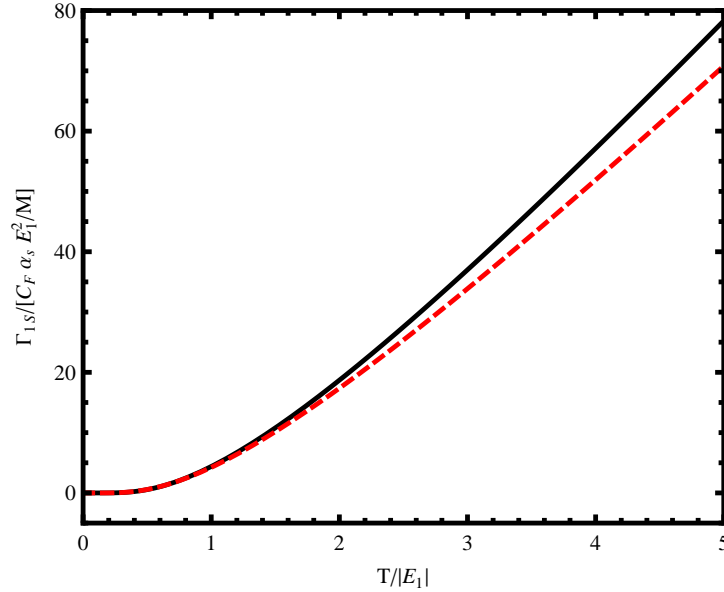

FIGURE 10. Exact gluodissociation width at leading order (continuous black line) vs the Bhanot–Peskin approximation (dashed red line).

CONCLUSIONS

We have studied the dissociation of quarkonium in a thermal bath of gluons and light quarks in a framework that makes close contact with modern effective field theories for non relativistic bound states at zero temperature. In a weakly-coupled framework, our conclusions may be concisely summarized in the following way.

(i) For $T < E_{\text{binding}}$ the quark-antiquark potential in the medium coincides with the potential at $T = 0$.

(ii) For $T > E_{\text{binding}}$ the potential gets thermal contributions.

(iii) For $m_D < E_{\text{binding}}$ quarkonium decays dominantly via gluodissociation (aka singlet-to-octet break up).

(iv) For $m_D > E_{\text{binding}}$ quarkonium decays dominantly via inelastic parton scattering (aka Landau damping).

(v) For $T \gtrsim T_{\text{dissociation}}(< T_{\text{screening}})$, quarkonium dissociates before forming.

In a strongly-coupled framework, the hierarchy of non-relativistic scales is preserved, whereas the thermodynamical hierarchy may break down. This requires a non-perturbative definition and evaluation of the potential (real and imaginary).

ACKNOWLEDGMENTS

REFERENCES

1. S. Biondini, talk at this conference.
2. M. Escobedo, talk at this conference.
3. N. Brambilla, J. Ghiglieri, A. Vairo and P. Petreczky, Phys. Rev. D **78**, 014017 (2008) [arXiv:0804.0993 [hep-ph]].
4. N. Brambilla *et al.*, CERN-2005-005, (CERN, Geneva, 2005) [arXiv:hep-ph/0412158].
5. N. Brambilla, S. Eidelman, B. K. Heltsley, R. Vogt, G. T. Bodwin, E. Eichten, A. D. Frawley and A. B. Meyer *et al.*, Eur. Phys. J. C **71**, 1534 (2011) [arXiv:1010.5827 [hep-ph]].
6. A. Bazavov *et al.* [HotQCD Collaboration], Phys. Rev. D **90**, 094503 (2014) [arXiv:1407.6387 [hep-lat]].
7. T. Matsui and H. Satz, Phys. Lett. B **178**, 416 (1986).
8. N. Brambilla, A. Pineda, J. Soto and A. Vairo, Rev. Mod. Phys. **77**, 1423 (2005) [hep-ph/0410047].
9. N. Brambilla, M. A. Escobedo, J. Ghiglieri, J. Soto and A. Vairo, JHEP **1009**, 038 (2010) [arXiv:1007.4156 [hep-ph]].
10. A. Vairo, AIP Conf. Proc. **1317**, 241 (2011) [arXiv:1009.6137 [hep-ph]].
11. W. E. Caswell and G. P. Lepage, Phys. Lett. B **167**, 437 (1986).
12. G. T. Bodwin, E. Braaten and G. P. Lepage, Phys. Rev. D **51**, 1125 (1995) [Erratum-ibid. D **55**, 5853 (1997)] [hep-ph/9407339].
13. A. Pineda and J. Soto, Nucl. Phys. Proc. Suppl. **64**, 428 (1998) [hep-ph/9707481].
14. N. Brambilla, A. Pineda, J. Soto and A. Vairo, Nucl. Phys. B **566**, 275 (2000) [hep-ph/9907240].
15. D. Kharzeev and H. Satz, Phys. Lett. B **334**, 155 (1994) [hep-ph/9405414].
16. X. M. Xu, D. Kharzeev, H. Satz and X. N. Wang, Phys. Rev. C **53**, 3051 (1996) [hep-ph/9511331].
17. L. Grandchamp and R. Rapp, Phys. Lett. B **523**, 60 (2001) [hep-ph/0103124].
18. L. Grandchamp and R. Rapp, Nucl. Phys. A **709**, 415 (2002) [hep-ph/0205305].
19. N. Brambilla, M. A. Escobedo, J. Ghiglieri and A. Vairo, JHEP **1305**, 130 (2013) [arXiv:1303.6097 [hep-ph]].
20. M. Laine, O. Philipsen, P. Romatschke and M. Tassler, JHEP **0703**, 054 (2007) [hep-ph/0611300].
21. M. A. Escobedo and J. Soto, Phys. Rev. A **82**, 042506 (2010) [arXiv:1008.0254 [hep-ph]].
22. A. Vairo, EPJ Web Conf. **71**, 00135 (2014) [arXiv:1401.3204 [hep-ph]].
23. N. Brambilla, M. A. Escobedo, J. Ghiglieri and A. Vairo, JHEP **1112**, 116 (2011) [arXiv:1109.5826 [hep-ph]].
24. F. Brezinski and G. Wolschin, Phys. Lett. B **707**, 534 (2012) [arXiv:1109.0211 [hep-ph]].
25. M. E. Peskin, Nucl. Phys. B **156**, 365 (1979).
26. G. Bhanot and M. E. Peskin, Nucl. Phys. B **156**, 391 (1979).